ELSEVIER

Journal of Organometallic Chemistry 637–639 (2001) 476–483

Journal of Organometallic Chemistry

www.elsevier.com/locate/jorganchem

Ferrocenyl naphthalene diimide can bind to DNA·RNA hetero duplex: potential use in an electrochemical detection of mRNA expression

Shinobu Sato [a], Satoshi Fujii [a], Kenichi Yamashita [a], Makoto Takagi [a], Hiroki Kondo [b], Shigeori Takenaka [a,*]

[a] *Department of Applied Chemistry, Faculty of Engineering, Kyushu University, Fukuoka 812-8581, Japan*
[b] *Department of Biochemical Engineering and Science, Kyushu Institute of Technology, Iizuka 820-8502, Japan*

Received 29 January 2001; received in revised form 17 February 2001; accepted 13 March 2001

Abstract

The novel ferrocenyl naphthalene diimide derivative **1** was synthesized by the condensation reaction between ferroceneacetic acid and terminal amino moieties of two imide substituents of naphthalene diimide. Stopped-flow analysis of the ligand **1** and DNA interaction revealed the following results: (i) the ligand binds to double stranded DNA more strongly than to single stranded DNA; (ii) the ligand does not have a bias against DNA sequence; (iii) the ligand can bind to the DNA·RNA hetero duplex more strongly than to the DNA·DNA duplex. These properties of **1** make it a suitable ligand for analysis of not only DNA but RNA. In fact, a current due to **1** was observed at 269 mV in the differential pulse voltammetric analysis of dA_{20}-immobilized electrode in an electrolyte containing **1**. The current increased markedly upon hybridization with polyU, whereas no current increase was obtained for polyA. Since the DNA·RNA hetero duplex is formed between sample RNA and DNA on the electrode, **1** may be used for the electrochemical detection of mRNA expression.

Keywords: Ferrocenyl naphthalene diimide; DNA·RNA hetero duplex; Electrochemical detection

1. Introduction

It is well known that ferrocene derivatives undergo reversible redox reactions in aqueous solution. This property of ferrocene has been exploited for various purposes [1]. Its use as a probe to detect the target gene electrochemically is a notable example [2,3]. We and others reported on a ferrocenyl oligonucleotide coupled with the HPLC-ECD system [4–6] or with a probe DNA-immobilized electrode for the sandwich DNA detection system [7]. We succeeded in DNA sensing by using ferrocenylnaphthalene diimide **2** coupled with a probe DNA-immobilized electrode [8–10]. This technique is based on the ability of **2** to discriminate double stranded DNA from single stranded DNA with a large margin. When a probe DNA immobilized on the electrode is allowed to hybridize with sample DNA in solution, a DNA duplex is formed on the electrode. Ligand **2** is concentrated on the electrode surface in proportion to the duplex region of DNA and gives rise to an electrochemical signal to allow DNA sensing. The rationale behind this idea is as follows. Ligand **2** acts as a threading intercalator where one of the substituents is lying in the major groove and the other in the minor groove in the complex with a DNA duplex. Therefore, these substituents serve as an anchor to prevent **2** from dissociating from double stranded DNA, whereas **2** dissociates readily from single stranded DNA because there is no stabilizing interaction between the two.

In light of the recent advent of DNA microarray and DNA chip technologies, it should be appropriate to apply the ferrocenyl ligand to the multi-electrode gene sensor as an electrochemical DNA chip, since the current chip technologies suffer several drawbacks such as the time required for analysis of multiple samples at a time. To circumvent these problems, we designed and synthesized a novel ferrocenyl naphthalene diimide **1** in

* Corresponding author. Fax: +81-92-642-3603.
E-mail address: staketcm@mbox.nc.kyushu-u.ac.jp (S. Takenaka).

0022-328X/01/$ - see front matter
PII: S0022-328X(01)00951-2

this paper, carrying ferrocene moieties at the end of linker chains from the naphthalene diimide skeleton. Since this ligand possesses methylene moieties instead of the carbonyl in **2**, it should give rise to a redox potential at the more negative side than that of **2**, resulting in the curtailment of the measuring time. In addition, it was found that **1** could bind to the DNA·RNA hetero duplex more strongly than to the DNA homo duplex. This property of the system can easily find use in mRNA expression analysis which is important in the post genome research.

2. Experimental

2.1. Chemicals

5′ - Mercaptohexyloligonucleotide, 5′ - $HS(CH_2)_6$ - pdA_{20}-3′, was obtained from Hokkaido System Sciences Co. Ltd. (Sapporo, Japan) and its concentration was estimated from the molar absorptivities at 260 nm [11]. Calf thymus DNA, $[poly(dA–dT)]_2$, $[poly(dG–dC)]_2$, polydT, polyApolyU, polyA, and polyU were purchased from Sigma–Aldrich Co. Calf thymus DNA was purified as described previously [12]. Denaturation of calf thymus DNA was carried out in aqueous solution by heating at 100 °C for 10 min and then immediately cooling on ice. The concentrations of polynucleotides were estimated from the molar absorptivities based on nucleic base: calf thymus DNA [13] and $[poly(dA–dT)]_2$ (6600 cm^{-1} M^{-1} at 262 nm) [14], $[poly(dG–dC)]_2$ (8400 cm^{-1} M^{-1} at 254 nm) [15], polydApolydT (6000 cm^{-1} M^{-1} at 260 nm) [15], polydT (8520 cm^{-1} M^{-1} at 264 nm) [16], polyApolyU (7300 cm^{-1} M^{-1} at 253 nm) [17], polyA (9800 cm^{-1} M^{-1} at 258 nm) [17], and polyU (9350 cm^{-1} M^{-1} at 260 nm) [17]. The DNA·RNA hetero duplex of polyApolydT was prepared by slowly cooling after heating the solution of an equimolar mixture of polyA and polydT.

2.2. Synthesis

Ferrocenyl naphthalene diimide **1** was synthesized according to the route given in Scheme 1. The structure of ligand **2** described previously [8–10] is also shown in Scheme 1.

2.2.1. *{3-[3-(Aminopropyl)methylamino]propyl}carbamic acid tert-butyl ester* ***(3)***

N,*N*′-bis(3-Aminopropyl)methylamine (20.6 ml, 0.10 mol) was dissolved in dioxane (45 ml). *S-tert*-butoxycarbonyl-4,6-dimethyl-2-mercaptopyrimidine [18] (12 g, 50 mmol) in dioxane (50 ml) was added slowly to the stirred solution over a period of 3 h, and the reaction was allowed to proceed overnight. The precipitate formed was removed by filtration, and the filtrate was evaporated. The subsequent addition of water (75 ml) precipitated bis-Boc product which was removed by filtration. The solvent was removed under reduced pressure and following the addition of 20 g of NaCl, the aqueous solution was extracted with ethyl acetate (50 ml each, four times). The organic phase was combined and evaporated under reduced pressure to give **3** as a yellow viscous oil: yield 3.76 g (25%); ^{1}H-MNR (400 MHz, $CDCl_3$) δ 1.44 (9H, s), 1.60 (4H, m), 2.40 (12H, m), 2.74 (2H, t), 3.17 (2H, t), 5.46 (1H, s) ppm.

2.2.2. *N,N′-bis[3-(3-tert-Butoxycarbonylaminopropyl)-methylaminopropyl]naphthalene-1,4,5,8-tetracarboxylic acid diimide, Boc naphthalene diimide derivative* ***(4)***

Naphthalene - 1,4,5,8 - tetracarboxylic dianhydride (0.62 g, 2.3 mmol) and mono-Boc amine **3** (3.5 g, 11.6 mmol) were refluxed in THF (15 ml) for 18 h. The solution was allowed to cool and then poured into chloroform (50 ml). The precipitate formed was removed by filtration, the filtrate poured into water (150 ml) and the solution was sonicated and kept at 2 °C for 1 h. The product was obtained as a pale brown solid: yield 1.2 g (62%); m.p. 115–120 °C; ^{1}H-NMR (400 MHz, $CDCl_3$) δ 1.43 (18H, s), 1.91 (4H, m), 2.31 (6H, m), 2.48 (6H, m), 3.18 (4H, t), 4.29 (4H, t), 5.46 (1H, s), 8.76 (4H, s) ppm.

2.2.3. *N,N′-bis[3-(3-Aminopropyl)methylaminopropyl]-naphthalene-1,4,5,8-tetracarboxylic acid diimide* ***(5)***

Boc naphthalene diimide derivative **4** (0.5 g, 0.6 mmol) was dissolved in trifluoroacetic acid (TFA) (4.3 ml, 58 mmol) and the solution was stirred for 1 h. The solid formed was filtered, re-dissolved in methanol (30 ml) and poured into $CHCl_3$ (350 ml) and kept at 4 °C overnight. The product was obtained as a pale pink solid, yield 0.76 g (97% as 6TFA salt).

2.2.4. *N,N′-bis[3-(3-Ferroceneacetylaminopropyl)-methylaminopropyl]naphthalene-1,4,5,8- tetracarboxylic acid diimide* ***(1)***

A solution of **5** (0.39 g, 0.40 mmol), ferroceneacetic acid (0.29 g, 1.2 mmol), 1-ethyl-3-(3-dimethylaminopropyl)carbodiimide, WSCI (0.23 g, 1.2 mmol) and triethylamine (0.5 ml) in $CHCl_3$ (3 ml) was stirred at room temperature (r.t.) for 17 h. The solvent was removed and the residue was chromatographed on a column of silica gel (Merck 60, methanol). The fraction showing a R_f of 0.17 on TLC (methanol) was collected, and the solvent was removed under reduced pressure. The residue was dissolved in a small amount of methanol and the resultant mixture was poured into water. The solid obtained by filtration was recrystallized from methanol and water to give 80 mg (20%) as a yellow solid, m.p. 159–160 °C; ^{1}H NMR (400 MHz, $CDCl_3$) δ 1.56–1.70 (8H, m), 1.78–1.92 (4H, m), 2.12

(6H, s), 2.33–2.46 (8H, m), 3.30–3.42 (4H, m), 3.36 (4H, s), 4.13 (10H, s), 4.20 (8H, s), 6.85 (2H, bs), 8.80 (4H, s) ppm; MS (time-of-flight mode with α-cyano-4-hydroxycinnamic acid as matrix) m/z [M + H] 975.46 (theory for $C_{52}H_{60}N_6O_6Fe_2 + H^+$ 975.763).

2.3. Stopped-flow analysis

SF-61 DX2 double mixing stopped-flow system (Hi-Tech Scientific Inc., UK) equipped with temperature controller Lauda RE206 was used for kinetic analysis of the DNA–intercalator interaction. The solution was prepared in morpholinoethanesulfonate (MES) buffer (10 mM MES, 1 mM EDTA, 0.1 M NaCl, pH 6.2). Observed association rate constants of the ligand with DNA were obtained by fitting the experimental data of absorption change after mixing with a 20-fold excess of DNA over intercalator to the equation of $A_1 \exp(k_1 t) + A_2 \exp(k_2 t)$, where A and k refer to the fractional amplitudes and rate constants, respectively, for the two-exponential fit to the results. Similar values were obtained by changing the molar ratio of DNA to **1** from 20 to 30. Intrinsic second-order association rate constant (k_a) and dissociation rate constant (k_d) were obtained from the slope of the plot of the apparent association rate constant (k_{app}) against DNA concentration based on the equation [19]: $k_{app} = k_a[DNA] + k_d$. The k_d was obtained from the y-intercept of the above plot, while the dissociation rate constant was obtained from the sodium dodecyl sulfate (SDS)-driven dissociation process. Thus, when the DNA–intercalator complex was mixed with a SDS solution, free intercalator was incorporated into the SDS micelle. Since this process is diffusion-controlled, the entire absorption change represents the k_d-dependent process and, therefore, the fitting of the kinetic trace provided the k_d value. Both k_d values from the intercept and the SDS-driven kinetics were in good agreement within error.

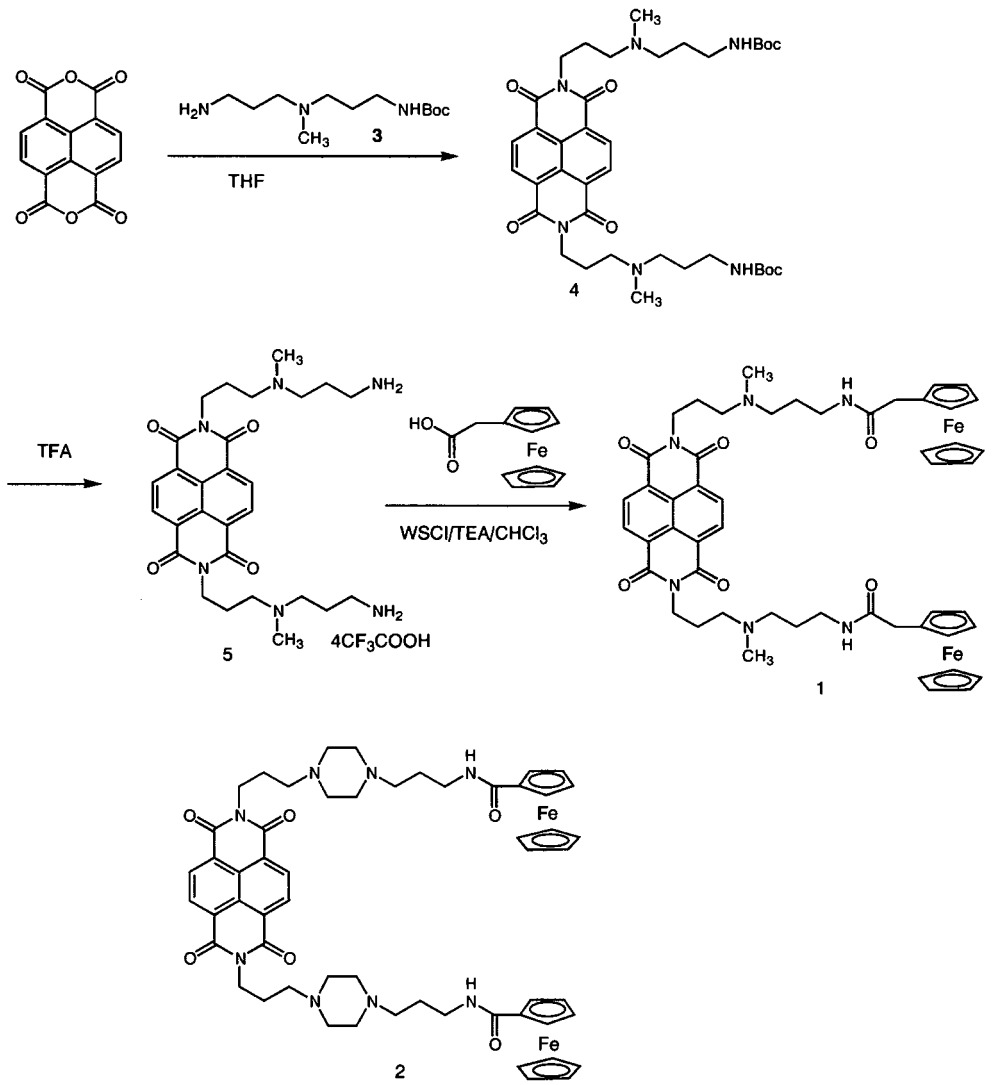

Scheme 1.

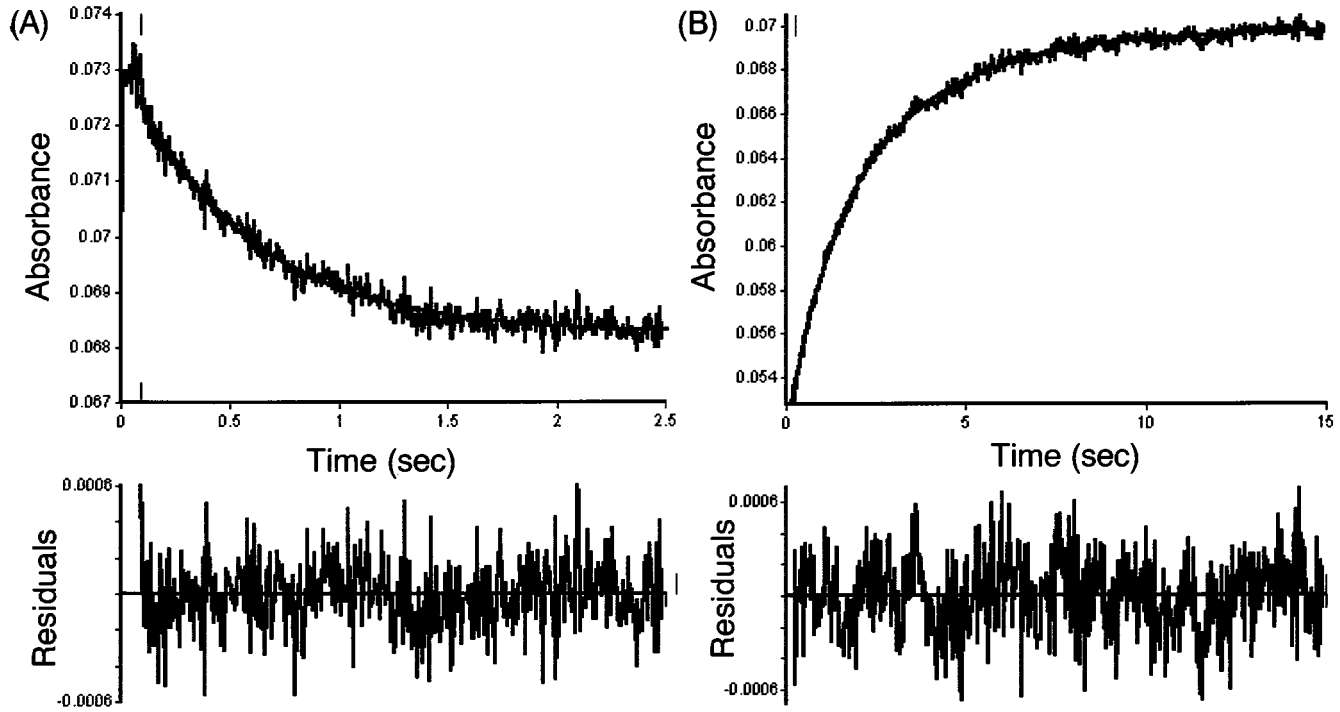

Fig. 1. Stopped-flow kinetic traces for the association (A) and the SDS-driven dissociation (B) for a complex of **1** with intact calf thymus DNA. The smooth line represents the two-exponential fit to the data. A residual plot for the fit is shown under the experimental plot. The experiments were conducted at 20 °C in MES buffer with 0.1 M NaCl at a ligand **1** to DNA base pair ratio of 1:20. The concentration of **1** was 5 μM.

The two-exponential equation rather than the single-exponential one was needed to obtain good fitting of the curve. The exact reason for this is not known, but the binding of the ligand from the major and minor grooves may not be equivalent.

2.4. Melting temperature (T_m) measurement

Absorption spectra were determined on a Hitachi U-3300 UV–vis spectrophotometer equipped with a temperature controller Hitachi SPR-10 (Hitachi Co. Ltd., Japan). In the melting curve experiments, a heating rate was set at 0.5 °C min^{-1}. The absorption based on nucleic base was monitored during this process.

2.5. Electrochemical measurements

This measurement was performed with ALS model 900 electrochemical analyzer (CH Instrument Inc., USA). Cyclic voltammetry (CV) and differential pulse voltammetry (DPV) were run at 25 °C with a normal three-electrode configuration consisting of an Ag/AgCl reference electrode, Pt counter electrode, and indicator electrode. 2-Mercaptoethanol-immobilized gold electrode was prepared by dipping in an aqueous solution containing 1 mM 2-mercaptoethanol for 1 h at 25 °C. A dA_{20}-immobilized gold electrode (1 pmol/2 mm^2) was prepared according to the procedure described previously [9]. Hybridization of dA_{20} on the electrode with polyU or polyA (20 pmol-base) was performed by incubation in the 2 × SSC for 1 h at 25 °C. All data were standardized using Δi values, defined as $(i/i_o - 1) \times 100\%$, where i_o and i refer to the current before and after hybridization, respectively. The Δi value represents a net increase in the current of the DNA·RNA hetero duplex formed per dA_{20}-immobilized electrode.

3. Results

3.1. Kinetic analysis

When ligand **1** was mixed with calf thymus DNA, its absorption at 383 nm decreased dramatically and shifted slightly toward the longer wavelength. This phenomenon is typical for threading intercalators such as substituted naphthalene diimides and it was used for kinetic analysis of DNA intercalation of **1**. Fig. 1 shows an example of the association and dissociation kinetic traces for the calf thymus DNA–**1** interaction. All data were analyzed by two-exponential fitting and the results are summarized in Table 1 for several nucleic acids in 10 mM morpholinoethanesulfonate (MES) and 1 mM EDTA (pH 6.2) containing 0.1 M NaCl. Precise kinetic analysis for single stranded nucleic acids of polydT, polyA, or polyU, was impossible, because the complex with either of them dissociated too fast (within 0.001 s). Analysis was possible with denatured calf thymus

Table 1
Kinetics and binding parameter of **1** with several nucleic acids

Nucleic acids	k_a (M^{-1} s^{-1})	k_d (SDS) (s^{-1})	K (M^{-1})
Calf thymus DNA	1.2×10^4	0.01	1.2×10^6
Denatured calf thymus DNA	1.8×10^5	13.0	4.2×10^4
$[poly(dA–dT)]_2$	1.4×10^5	2.3	0.6×10^5
$[poly(dG–dC)]_2$	1.4×10^4	0.1	1.4×10^5
polydApolydT	–	3.6	–
polydT	–	>200	–
polyApolyU	–	60.1	–
polyA	–	>200	–
polyU	–	>200	–
polyApolydT	2.8×10^5	0.62	4.5×10^5

Experiments were conducted at 25 °C 10 mM MES, 1 mM EDTA (pH 6.2) containing 0.1 M NaCl; k_d (SDS) were obtained from the SDS-driven dissociation analysis; –: not determined.

DNA, but this DNA is a variable mixture of double stranded and single stranded DNA. With this situation of denatured calf thymus DNA in mind, the binding constant K of **1** with intact DNA was determined to be 33 times larger than that with the denatured, and the k_d of **1** for intact DNA is 1900 times smaller than that for the denatured. The binding constants for $[poly(dA–dT)]_2$ and $[poly(dG–dC)]_2$ were identical (10^5 M^{-1}), though both the association and dissociation processes for $[poly(dG–dC)]_2$ were 10–20 times slower than those for $[poly(dA–dT)]_2$. This result is reasonable in light of the fact that ligand **1** acts as a threading intercalator to allow one of its substituents to penetrate into base pairs of the DNA duplex and that the breathing rate of GC base pairs is smaller than that of AT base pairs [20]. In other words, ligand **1** does not discriminate DNA base pairs nor sequences. This property of **1** is suitable as a DNA probe. Association rate constants of **1** with polydApolydT and polyApolyU were not obtained, because both processes occurred too fast with either of them, though the binding constants seemed not to be different much from those for other nucleic acids. The binding constant of **1** for polyApolydT as the DNA·RNA hetero duplex was 4 times larger than that for $[poly(dA–dT)]_2$ or $[poly(dG–dC)]_2$, demonstrating that ligand **1** can bind to hetero duplexes more preferably, whereas classical intercalators such as ethidium bromide show decreased binding affinity for them [21].

3.2. Correlation between T_m and the DNA–intercalator interaction

Melting temperature curves of nucleic acids were measured in the same buffer as that for the kinetic studies and the T_m is plotted against the k_a values in Fig. 2. Inverse correlation was observed between k_a and T_m. The T_m values are supposed to correlate with the DNA breathing [22] and therefore the association process of **1** with nucleic acids also depends on it. In other words, the association rate represents the frequency of breathing of DNA so as to allow one of the substituents of the intercalator to penetrate into the base pairs of DNA duplex.

3.3. Electrochemical behavior

First of all, CV was measured with the plain gold electrode in 0.1 M AcOH–AcOK buffer (pH 5.6) containing 0.1 M KCl and 0.05 mM **1**. There was a large conducting component observed, which seemed to derive from the absorption of naphthalene diimide part of **1**, preferentially on the surface of the electrode. Such undesired absorption was blocked by 2-mercaptoethanol coating of the electrode. Fig. 3 shows a CV of a solution of **1** or **2** measured with a 2-mercap-

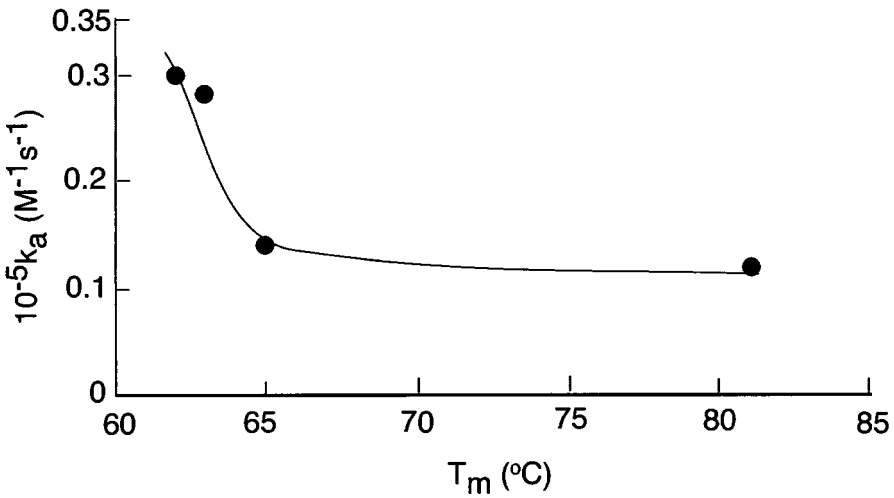

Fig. 2. Correlation between T_m and k_a for the complex of **1** with several nucleic acids. The T_m was measured under the same conditions as those of kinetic analysis except for the absence of **1**.

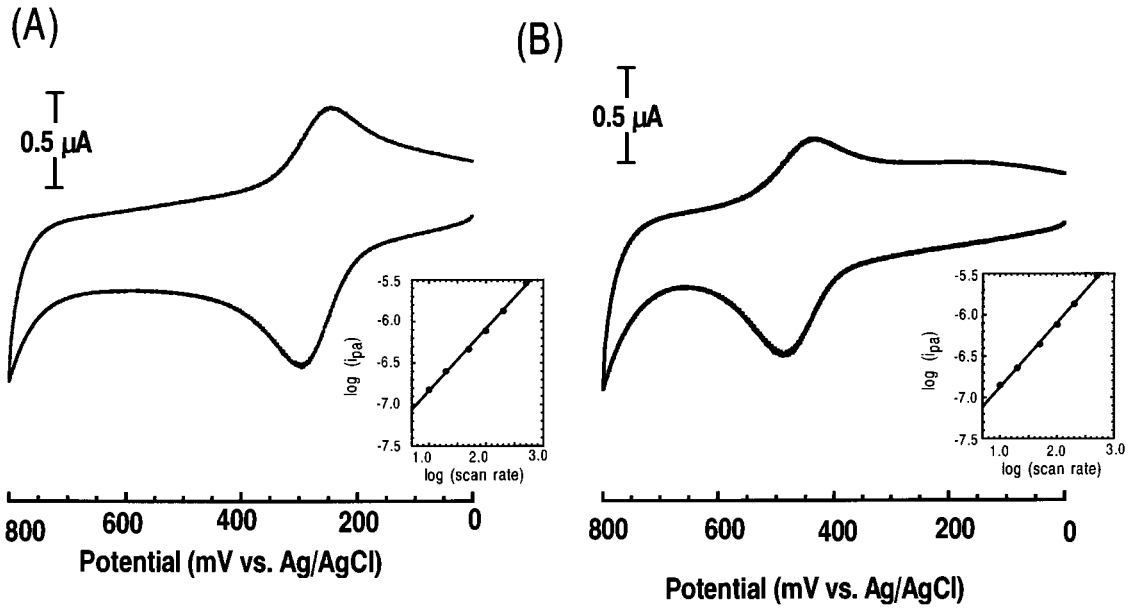

Fig. 3. Cyclic voltammograms of **1** and **2** on a 2-mercaptoethanol-immobilized gold electrode.

toethanol-immobilized gold electrode in 0.1 M AcOH–AcOK buffer (pH 5.6) containing 0.1 M KCl and 0.05 mM **1** or **2**. A one-step redox reaction of the ferrocene moiety of **1** was observed on the positive side ($E_{1/2} =$ 269 mV, $\Delta E_p = 50$ mV), whereas that for **2** was observed on the more positive side ($E_{1/2} = 489$ mV, $\Delta E_p = 50$ mV). This was exactly what was expected, as the linkers between the ferrocene and the amino moieties of **1** are electron-donating methylenes, while that of **2** is an electron-withdrawing carbonyl. Therefore, the ferrocene of **1** is rendered more electron-rich than that of **2** and the redox potential of **1** shifted to the negative side from that for **2** reported previously [9]. Both ΔE values of **1** and **2** were 50 mV, in contrary to 59 mV in theory. To clarify this anomaly, the logarithm of the cathodic current was plotted against the logarithm of the scan rate for the individual peaks of **1** and **2** (Fig. 3). The slope obtained of 0.8 suggests that an absorption process contributes significantly to the electron transfer reaction in both cases.

Fig. 4 depicts DPV curves for **1** centered at 290 mV before and after hybridization of polyU or polyA with a dA_{20}-immobilized electrode. The current increased markedly for the complementary polyU with a mean Δi of 112.9% and a standard deviation of 18.7% for five measurements ($n = 5$), while the current for the non-

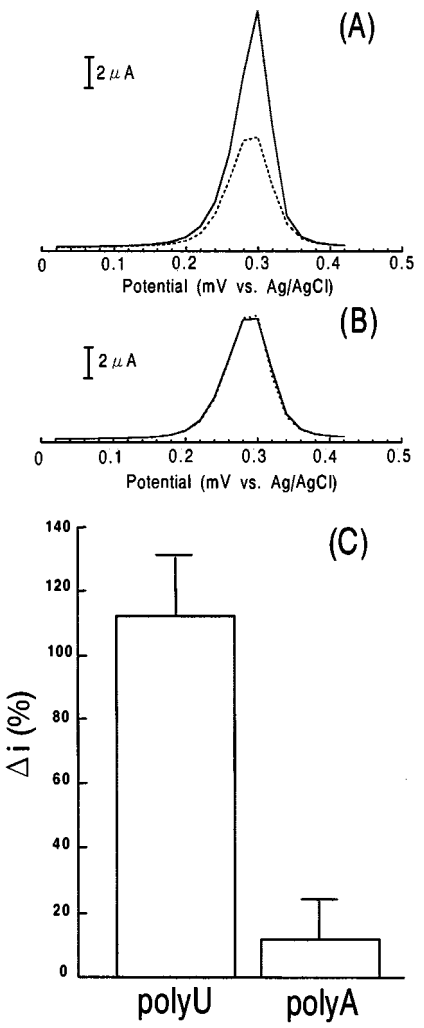

Fig. 4. Differential pulse voltammograms of a dA_{20}-immobilized gold electrode before (broken line) and after hybridization (solid line) with polyU (A) or polyA (B) in an electrolyte containing 0.05 mM **1**. (C) Δi values for the complementary (polyU) and non-complementary (polyA) combinations with a respective mean and standard deviation of 112.9, 18.7, 11.9 and 12.6%.

complementary polyA was barely above background with the corresponding values of 11.9 and 12.6% (Fig. 4c).

3.4. Computer modeling

The complex structure of an anthraquinone derivative intercalator and oligonucleotide d(AAATTT)$_2$ duplex was obtained from the PDB database and the initial structure of the complex was constructed by replacing **1** for anthraquinone and then optimized by molecular mechanics using Insight II (Molecular Simulation Inc., USA). The sturucture of the complex of **1** with d(AAATTT)$_2$ duplex thus obtained is depicted in Fig. 5. The amino moieties of **1** are located near the phosphate anion side of DNA, presumably through electrostatic interactions, and the ferrocene moieties are located in the major and minor grooves of DNA duplex simultaneously.

4. Discussion

As described above, novel ferrocenyl naphthalene diimide **1** exhibits a better property than **2** with respect to DNA detection. For one thing, the peak response of **1** appeared at 269 mV in DPV, shifted toward the negative side by 220 mV from that of **2**. Since the voltage is applied from zero toward the peak in DPV measurements, the time to complete the scan with ligand **1** is shortened to 4 s from 6 s with **2**. This characteristic of **2** relates to the following advantages: (i) the lower redox potential can suppress cleavage of the gold-sulfur linkage and detachment of the DNA probe from the gold electrode; and (ii) the time to complete the scan from zero voltage with ligand **1** is shortened to 4 s from 6 s with **2** (DPV measurements can be started from any voltage in principle. However, non-Faraday current increases at a higher potential and hence a longer quite time is inevitable to result in a

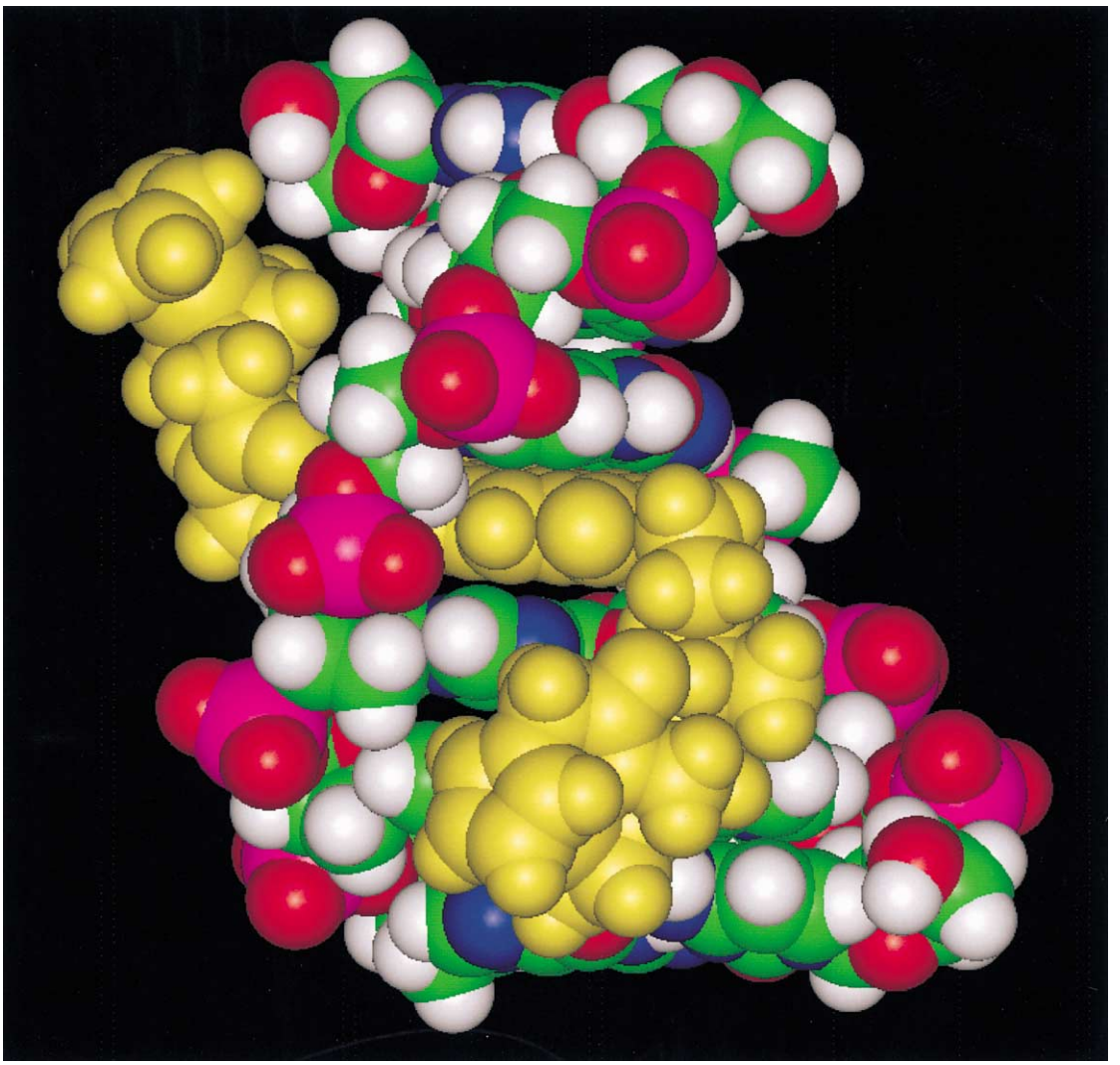

Fig. 5. An Insight II molecular mechanics representation of the threading intercalation complex of **1** with d(AAATTT)$_2$ duplex.

longer overall measurement time). Although this change is modest, it will amount to a significant curtailment of measurement time with multi-electrode gene sensors, which handle multiple samples sequentially. Another characteristic of ligand **1** is that the specificity for double stranded DNA was improved considerably. Thus, **1** binds to double stranded DNA 33 times more strongly than single stranded (Table 1), as compared with the five times with **2**. The third characteristic, though not specific to **1** but shared by **2**, is that it hardly has a bias against base pair or sequence, resulting in its indiscriminate binding to double stranded DNA irrespective of base composition and sequence. All of these properties makes **1** an ever more suitable ligand for DNA analysis.

In addition to these features, **1** exhibits preference for DNA·RNA hetero duplexes to DNA·DNA homo duplexes. In general, the DNA duplex adopts a B form with its nucleic base pairs kept planar [23]. Therefore, classical intercalators are able to creep between nucleic bases without inducing their large conformational change [24]. On the other hand, the DNA·RNA hetero duplex adopts an A form-like structure and its base pairs are bent with some angles from the plane to assume a propeller-twist conformation [25]. Therefore a structural change is required for the A form duplex to accommodate (classical) intercalators [26], thereby making this process less favorable energetically. By contrast, threading intercalators can penetrate the (hetero) duplex without inducing its conformational change and their terminal bulky substituents serve as an anchor to prevent the complex from dissociating. Hence, threading intercalators are able to stabilize the complex of homo and hetero duplexes equally well. In addition, the association process of threading intercalators to hetero duplexes may be facilitated further because of the large minor groove of the DNA·RNA duplex available for intercalation [25]. This additional advantage may have led to the observed increase in the affinity of **1** for the hetero duplex. These behavior of **1** is suitable for the detection of mRNA with a probe DNA-immobilized electrode, where a DNA·RNA hetero duplex is formed between the target mRNA and the probe DNA. Our preliminary electrochemical experiments on mRNA analysis demonstrated that ligand **1** works as well as in DNA sensing. An expression analysis of mRNA from the *Lac Z* gene of *Escherichia coli* was successful in this system (unpublished observation).

Acknowledgements

This work was supported in part by a grant-in-aid for Scientific Research from the Ministry of Education, Science and Culture, Japan. The authors are also grateful for a financial support from the New Energy and Industrial Technology Development Organization (NEDO) of Japan.

References

[1] I. Willner, E. Katz, Angew. Chem. Int. Ed. Engl. 39 (2000) 1180.
[2] R.C. Mucic, M.K. Herrlein, C.A. Mirkin, R.L. Letsinger, Chem. Commun. (1996) 555.
[3] S.M. Waybright, C.P. Singleton, J.M. Tour, C.J. Murphy, U.H. Bunz, Organometallics 19 (2000) 368.
[4] S. Takenaka, Y. Uto, H. Kondo, T. Ihara, M. Takagi, Anal. Biochem. 218 (1994) 436.
[5] T. Ihara, Y. Maruo, S. Takenaka, M. Takagi, Nucleic Acids Res. 24 (1996) 4273.
[6] Y. Uto, H. Kondo, M. Abe, T. Suzuki, S. Takenaka, Anal. Biochem. 250 (1997) 122.
[7] T. Ihara, M. Nakayama, M. Murata, K. Nakano, M. Maeda, J. Chem. Soc. Chem. Commun. (1997) 1609.
[8] S. Takenaka, Y. Uto, H. Saita, M. Yokoyama, H. Kondo, W.D. Wilson, J. Chem. Soc. Chem. Commun. (1998) 1111.
[9] S. Takenaka, K. Yamashita, M. Takagi, Y. Uto, H. Kondo, Anal. Chem. 72 (2000) 1334.
[10] K. Yamashita, M. Takagi, H. Kondo, S. Takenaka, Chem. Lett. (2000) 1038.
[11] C.R. Cantor, M.M. Warshaw, Biopolymers 9 (1970) 1059.
[12] M.W. Davidson, B.G. Griggs, D.W. Boykin, W.D. Wilson, J. Med. Chem. 20 (1997) 1117.
[13] W. Muller, D.M. Crothers, Eur. J. Biochem. 54 (1975) 267.
[14] R.B. Inman, R.L. Baldwin, J. Mol. Biol. 5 (1962) 172.
[15] R.D. Wells, J.E. Larson, R.C. Grant, B.E. Shortle, C.R. Cantor, J. Mol. Biol. 54 (1970) 465.
[16] P.O.P. Tso, S.A. Rapaport, F.J. Bollum, Biochemistry 5 (1966) 4153.
[17] Pharmacia Biotech Catalogue.
[18] G.L. Stahl, R. Walter, C.W. Smith, J. Org. Chem. 43 (1978) 2285.
[19] F.A. Tanious, S.-F. Yen, W.D. Wilson, Biochemistry 30 (1991) 1813.
[20] P.H. von Hippel, K.-Y. Wong, J. Mol. Biol. 61 (1971) 587.
[21] To the authors' knowledge, the interaction of intercalators with DNA·RNA hetero duplexes has never been studied. Therefore, to estimate the stability of the complex between polyApolydT and ethidium bromide or **1**, the effect of the ligand on the T_m of the hetero duplex was measured in 10 mM MES buffer and 1 mM EDTA (pH 6.2) containing 1 mM NaCl. The ΔT_m, defined by the difference in T_m in the presence and absence of the ligand, of **1** was 20 °C, whereas that of ethidium 16 °C. This result implies that the threading intercalator stabilized its complex with the hetero duplex more effectively than the classical intercalator.
[22] M.P. Printz, P.H. von Hippel, J. Mol. Biol. 53 (1965) 363.
[23] S. Arnott, R. Chandrasekaran, D.W. Hukins, P.J.C. Smith, L. Watts, J. Mol. Biol., 88 (1974) 523.
[24] S. Arnott, D.W.L. Hukins, S.D. Dover, W. Fuller, A.R. Hodgson, J. Mol. Biol. 81 (1973) 107.
[25] W. Saenger, Principles of Nucleic Acid Structure, Springer-Verlag, New York, 1984.
[26] W.D. Wilson, L. Ratmeyer, M. Zhao, D. Ding, A.W. McConnaughie, A. Kumar, D.W. Boykin, J. Mol. Recog. 9 (1996) 187.